

Modeling, impact evaluation, and optimization of machining performances of heat-treated SKD61 steel in a tungsten powder alloy mixed EDM process via the RSM-GRA methodology

Van-Tao Le^{1,*}, Tien Long Banh², Thi Hong Minh Nguyen², Tien Dung Hoang³, Van Thuc Dang¹, Hoang Cuong Phan¹

¹Advanced Technology Center, Le Quy Don Technical University, Hanoi, Viet Nam

²School of Mechanical Engineering, Hanoi University of Science and Technology, Hanoi, Vietnam;

³Faculty of Mechanical Engineering, Hanoi University of Industry, Ha Noi, Viet Nam

Correspondence

Van-Tao Le, Advanced Technology Center, Le Quy Don Technical University, Hanoi, Viet Nam

Email: levantao@lqdtu.edu.vn

History

- Received: 2023-12-04
- Accepted: 2023-12-28
- Published Online: 2023-12-31

DOI :

<https://doi.org/10.32508/stdj.v26i4.4222>



Copyright

© VNUHCM Press. This is an open-access article distributed under the terms of the Creative Commons Attribution 4.0 International license.



ABSTRACT

Introduction: The use of conductive powders in electrodischarge machining (EDM) holds great potential for improving the machining process. This study investigated the addition of tungsten powder alloy to a dielectric liquid during an EDM process called powder mixed EDM (PMEDM) to process heat-treated SKD61 steel. The aim of this study comprises (i) considering the influence of essential process parameters, including pulse-on time (T_{on}), peak current (I_p), and amount of powder (A_p), on tool wear rate (TWR) and material removal rate (MRR) and (ii) finding an optimized coalescence of process variables for enhancing the MRR and reducing the TWR. **Methods:** For this purpose, the Box–Behnken matrix was adopted for the experimental design to obtain empirical data. Subsequently, adequate mathematical models and analysis of variance (ANOVA) for MRR and TWR were used to assess the adequacy of these models. Finally, gray relational analysis (GRA) was adopted for multiattribute optimization. **Results:** The results revealed that the I_p had the most robust influence on the MRR and TWR. However, the factors influencing TWR are A_p and T_{on} , while the reverse is true for MRR. The predictive models of MRR and TWR were constructed and validated for adequacy/precision through coefficients (comprising \hat{R}^2 , $\hat{R}^2(\text{pred})$, and $\hat{R}^2(\text{adj})$). From the predictive models, the optimal responses and process variables, including MRR_{max} of 0.003397818(g/min), TWR_{min} of 0.000481408(g/min), peak-current of 5(A), pulse-on time of 150(μ s), and powder concentration of 15(g/l) were found. In addition, microdefects at the optimum electrical mode were compared between the powder mode and the no-powder mode. As a result, the surface obtained with the powder mode has fewer microcracks, voids, droplets, and smaller globules of debris than the surface obtained with the powderless mode. **Conclusions:** The results of this study were obtained by evaluating the influence of process parameters on machining performance, establishing a prediction model for machining performance, and optimizing process parameters; these results can be applied in factual mold manufacturing and help technologists and researchers make the most suitable choices. In addition, the methods applied in this study can be applied in the PMEDM process to study different powders and workpiece materials.

Key words: EDM, PMEDM, tungsten powder alloy, MRR, TWR

INTRODUCTION

Powder mixed into electrodischarge machining (PMEDM) was developed based on electrodischarge machining, and PMEDM has emerged as a potential machining method for enhancing machining performance and surface quality to process cut-difficult materials and ensure the execution of complex shapes^{1,2}. PMEDM was born approximately four decades ago, and different powders were investigated. The influence of powders such as C, Fe, Cu, and Al on discharge properties, machining efficiency, and surface quality was first reported in 1981 by Erden *et al.*³. Subsequently, different powders, such as Si, SiC, Gr, Mo, Cr, Ti, TiC, Al, Ni, and C, were

investigated for their ability to enhance machining properties and surface quality⁴. However, few studies on tungsten powder alloys subjected to EDM have been performed.

The types of materials used during the EDM process were also investigated with various powders, including SS304, Ti64, AISI D2 steel, AISI W1 steel, SKD61 steel, and AISI P20 steel, which are regularly used in industry. SKD61 steel is a kind of tool steel. In particular, its mechanical properties are evaluated to be superior to those of other steels treated with heat⁵⁻⁷. In the manufacturing sector, heat-treated SKD61 steel is applied in hot stamping dies, blow molds, plastic molds, etc.⁸. However, other machining methods, such as turning and milling, have difficulty cut-

Cite this article : Le V, Banh T L, Nguyen T H M, Hoang T D, Dang V T, Phan H C. **Modeling, impact evaluation, and optimization of machining performances of heat-treated SKD61 steel in a tungsten powder alloy mixed EDM process via the RSM-GRA methodology.** *Sci. Tech. Dev. J.* 2023; 26(4):3150-3160.

ting and obtaining low efficiency when this material is machined in the heat-treated state. The electrochemical discharge (EDM) method has emerged as a potential machining method for this material state¹. With respect to SKD61 steel, there are several studies on this material with different powders. For instance, the surface attributes of SKD61 steel, including the surface roughness and thickness of the recast layer, were explored under conditions of EDM with added Al and surfactant powders⁹. The results revealed that the impact of Al and surfactant powders on the surface roughness (SR) and thickness of the recast layer is meaningful for improving the surface roughness. Another study of SKD61 steel with Cr and Al added to various dielectrics was reported¹⁰. This study revealed that factors such as peak current, pulse-on time, dielectric type, grain size, and the ratio of Al to Cr powder influenced the material removal rate (MRR), tool wear rate (TWR), SR, and microhardness (MH). Recently, tungsten carbide powder was investigated during EDM by Le *et al.*^{11,12}. These investigations have comprehensively explored surface attributes such as variations in compositional chemistry, SR, microcracks, MH, and the generation of alloy phases in surface layers and considered the electrical parameter domains where this powder has a positive or negative effect on surface modification. However, the material state of the abovementioned studies is the non-heat-treated state. Moreover, heat-treated SKD61 steel is commonly processed by the EDM method before further operation to obtain the complete set of molds.

As mentioned above, most of these investigations involve heat-untreated SKD61 steel, which is not amenable to practical manufacturing. Moreover, heat-treated SKD61 steel is commonly processed by the EDM method before further operation to obtain a complete mold set. In addition, in this study, the EDM process combined with tungsten compound powder suspended in an insulating solution has practical significance. Tungsten has very good physical and chemical properties at high temperatures when penetrating the surface. However, to date, this issue has received little attention from the research community. To fill the missing gap with tungsten powder alloy in the EDM process used to process heat-treated SKD61 steel, the obtained results provide and enrich necessary insights for the research community and are applied in the mold and component manufacturing industry. Hence, this study focused on developing predictive models of machining efficiency (TWR and MRR) by utilizing response surface methodology (RSM) for the machining of heat-treated SKD61 steel

by an EDM process with the addition of a tungsten powder alloy. From the obtained prediction models, the impact of crucial process parameters on machining performance can be analyzed and evaluated. Additionally, RSM-Gray relational analysis (GRA) was performed to determine the optimal machining performance, which helps technologists and researchers determine the proper option in the manufacturing sector.

MATERIALS AND METHODS

In **Figure 1b**, entire SKD61 steel specimens were machined to a size of 45x19 mm (height × diameter) with the nominal compositional chemistry given as 0.4Mn, 0.38C, 1 V, 1Si, 1.25Mo, 5Cr, and balanced Fe (in wt. %), and heat was applied to achieve a hardness of 50±2HRC. The trials were implemented on an EDM machine (CNC-460)-Aristech brand, and a reverse electrode of copper (99%Cu) was applied as a tool, as indicated in **Figure 1a** and **Figure 1c**. The grain size of the tungsten powder alloy is less than 31 μm, and the titular compositional chemistry is 82.5 W-11.9Co-5.56C- 0.02Fe-0.02 other composition (wt.%), which was evenly mixed into the dielectric fluid (EDM fluid 2 from Shell Company), as indicated in **Figure 1d** and **Figure 1e**.

The peak current (I_p) and pulse-on time (T_{on}) of the EDM process strongly influence the machining performance⁹. Therefore, I_p and T_{on} were considered to have a priming effect on machining performance, while the pulse-off time and current-voltage were held constant at 120 V and 50 μs, respectively. In addition, the amount of powder (A_p) also has a significant impact on machining performance. Hence, the essential parametric variables, namely, T_{on} , I_p , and A_p , were investigated in the experimental design. The empirical strategy was conducted on the Box–Behnken plot of the RSM to reduce the number of experiments and reduce the empirical cost. Compared to other empirical statistical methods, the capability of Box–Behnken is to construct accurate models, the most preferable of which involve three factors and levels¹³. The levels of the machining parameters are described in **Table 1**. The selection of the levels of I_p and T_{on} was dependent on the specifics of the CNC-460 EDM machine, according to prior works^{9,12,14} and pilot trials. The levels of A_p were based on pilot experiments and the thermal and electrical attributes of the powders.

MRR&TWR: MRR and TWR are computed by Eqs. (1) and (2), respectively. Here, W_1 and W_2 are the initial and finishing weights of the workpiece, respectively, and w_1 and w_2 are the tool electrode (g), respectively. The weights of the specimen and electrode

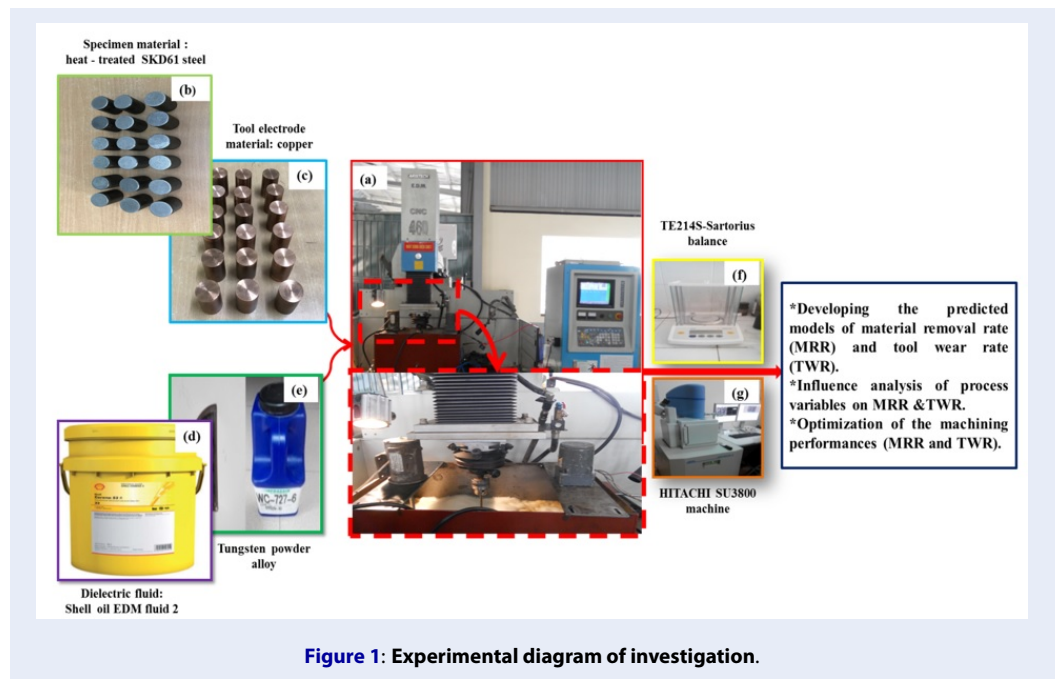


Figure 1: Experimental diagram of investigation.

Table 1: The levels of process parameters

Variables of process parametric	Levels		
I_p (A)	5	7	9
T_{on} (μs)	50	100	150
A_p (g/l)	0	15	30

were balanced by a Sartorius balance with respect to the TE214S code (a readability of 0.0001 g), as depicted in Figure 1f. The processing time in equations (1) and (2) is the duration needed to mutate the height of the samples from 45 mm down to 44.3 mm.

$$MRR \left(\frac{g}{min} \right) = \frac{W_1 - W_2}{processing\ time} \quad (1)$$

$$TWR \left(\frac{g}{min} \right) = \frac{w_1 - w_2}{processing\ time} \quad (2)$$

Surface defects: The microdefects on the surfaces obtained by PMEDM and EDM were explored on a HITACHI SU3800 machine by emission scanning electron microscopy (SEM), as indicated in Figure 1g.

Matrix of empirical variables and achieved output attributes: The empirical matrix of the machining variables and achieved data of attributes are described in Table 2. The trial matrix with the parametric variables and response data is described in Table 2 and was used to establish the regression model for MRR and TWR. Furthermore, four extra runs (from 16 to 19) were utilized to assess the precision of the development models. At each technological regime, the sample and electrode were measured three times before

and after machining. The average values were taken, and the results are shown in Table 2.

RESULTS

Establishing the prediction models

The prediction models of the output features, including the MRR and TWR, were established. A regression model of the quadratic equation was constructed, as delineated by Eq. (3):

$$f(x) = \lambda_0 + \sum_{i=1}^n \lambda_i x_i + \sum_{i=1}^n \lambda_{ii} x_i^2 + \sum_{i < j} \sum_{j=2}^n \lambda_{ij} x_i x_j \quad (3)$$

where λ_0 , λ_i , λ_{ii} , and λ_{ij} are the coefficients of the regression models; x_i and x_j are process parameters; the variable number is n, with n = 3; and the output property is $f(x)$ - i.e., MRR or TWR. In this study, the coefficients, regression models and analysis of variance (ANOVA) were computed and established with Minitab 19 software. The adequacy of the predictive models for MRR and TWR are delineated in the equations. (4) and (5), respectively, while the ANOVAs for

Table 2: Trial matrix and data of output

Run	Process parameters			Output variables	
	T_{on} -m	I_p -A	A_p -g/l	TWR- g/min	MRR- g/min
Empirical data for developing models					
1	50	9	15	0.001176108	0.003996503
2	50	5	15	0.000578622	0.001972537
3	100	9	30	0.001093224	0.003972222
4	100	7	15	0.000714120	0.002743987
5	100	7	15	0.000702218	0.002687734
6	150	9	15	0.000999094	0.004013167
7	50	7	30	0.000807356	0.002480000
8	100	5	30	0.000651593	0.002678663
9	50	7	0	0.000534151	0.001986364
10	100	9	0	0.000927740	0.003536138
11	150	7	30	0.000610508	0.003543158
12	100	5	0	0.000410404	0.002340698
13	100	7	15	0.000709320	0.002629356
14	150	7	0	0.000572218	0.002596923
15	150	5	15	0.000481408	0.003397818
Empirical data for testing accuracy of models					
16	50	5	30	0.000658931	0.001913934
17	150	7	15	0.000609828	0.003084515
18	100	7	30	0.000775432	0.002704641
19	150	9	30	0.000977515	0.004504535

MRR and TWR are described in the corresponding **Table 3** and **Table 4**:

$$MRR = 0.004438 + 0.000023T_{on} - 0.001332I_p + 0.000014A_p - 3.52154 \times 10^{-6} T_{on}I_p + 1.50866 \times 10^{-7} T_{on}C_p + 8.17656 \times 10^{-7} I_pC_p + 0.000142I_p^2 + 3.55322 \times 10^{-8} T_{on}C_p^2 + 5.52202 \times 10^{-7} A_p^2 \quad (4)$$

$$TWR = 0.000829 + 3.06562 \times 10^{-6} T_{on} - 0.000261I_p + 0.000026A_p - 1.995 \times 10^{-7} T_{on}I_p - 6.30875 \times 10^{-7} I_pA_p - 7.83051T_{on}A_p - 7.88531 \times 10^{-9} T_{on}^2 + 0.00003I_p^2 - 2.56805 \times 10^{-7} A_p^2 \quad (5)$$

Influential exploration of the manufacturing process variables on the MRR&TWR

The main impacts of single processing parameters on the MRR and TWR are described in the **Figure 2a** and **Figure 2b**, respectively. Moreover, the combined impacts of the machining variables on the MRR and TWR are depicted in the **Figure 3a-c** and **Figure 4a-c**, respectively. The pairs of factors considered for the

combined impact on MRR and TWR in this study included I_p and T_{on} , I_p and A_p , and T_{on} and A_p . The results (as indicated in **Table 3** and **Table 4**) revealed that I_p had the most robust influence on the MRR and TWR. However, the factors influencing TWR are A_p and T_{on} , while the reverse is true for MRR.

Validation of the computational models

In this investigation, the empirical data from 16 to 19 (as indicated in **Table 2**) were compared with the predictive data at the same processing parameters (as depicted in **Table 5**) to evaluate the accuracy of the proposed models. These results indicated that the percentage deviations of the TWR and MRR were 3.08% to 4.97% and 2.55% to 4.75%, respectively.

Table 3: ANOVA for the predictive model of the MRR

Source	Sum of Squares	Mean Square	p value	F value	Remark	Contribution
Model	6.976E-06	7.751E-07	0.0002	54.19	significant	
I_p	3.287E-06	3.287E-06	< 0.0001	229.81	significant	46.64%
T_{on}	1.213E-06	1.213E-06	0.0003	84.82	significant	17.22%
A_p	6.127E-07	6.127E-07	0.0012	42.83	significant	8.69%
$I_p \times T_{on}$	4.961E-07	4.961E-07	0.0020	34.68	significant	7.04%
$I_p \times A_p$	2.407E-09	2.407E-09	0.6987	0.1683	not significant	0.03%
$T_{on} \times A_p$	5.121E-08	5.121E-08	0.1170	3.58	not significant	0.73%
I_p^2	1.196E-06	1.196E-06	0.0003	83.61	significant	17.31%
T_{on}^2	2.914E-08	2.914E-08	0.2129	2.04	not significant	0.51%
A_p^2	5.700E-08	5.700E-08	0.1024	3.98	not significant	0.81%
Lack of Fit	6.495E-08	2.165E-08	0.1346	6.59	not significant	0.92%
"R ² " = 0.9899, "R ² (adj)" = 0.9716, and "R ² (pred)" = 0.8504						

Table 4: ANOVA for the predictive model of the TWR

Source	Sum of Squares	Mean Square	p value	F value	Remark	Contribution
Model	7.145E-07	7.939E-08	0.0001	67.05	significant	
I_p	5.378E-07	5.378E-07	< 0.0001	454.18	significant	74.65%
T_{on}	2.344E-08	2.344E-08	0.0067	19.79	significant	3.25%
A_p	6.447E-08	6.447E-08	0.0007	54.45	significant	8.95%
$I_p \times T_{on}$	1.592E-09	1.592E-09	0.2986	1.34	not significant	0.22%
$I_p \times A_p$	1.433E-09	1.433E-09	0.3214	1.21	not significant	0.2%
$T_{on} \times A_p$	1.380E-08	1.380E-08	0.0190	11.65	significant	1.92%
I_p^2	5.314E-08	5.314E-08	0.0011	44.88	significant	8.16%
T_{on}^2	1.435E-09	1.435E-09	0.3211	1.21	not significant	0.12%
A_p^2	1.233E-08	1.233E-08	0.0233	10.41	significant	1.71%
Lack of Fit	5.848E-09	1.949E-09	0.0181	54.37	significant	0.81%
"R ² " = 0.9918, "R ² (adj)" = 0.977, and "R ² (pred)" = 0.8699						

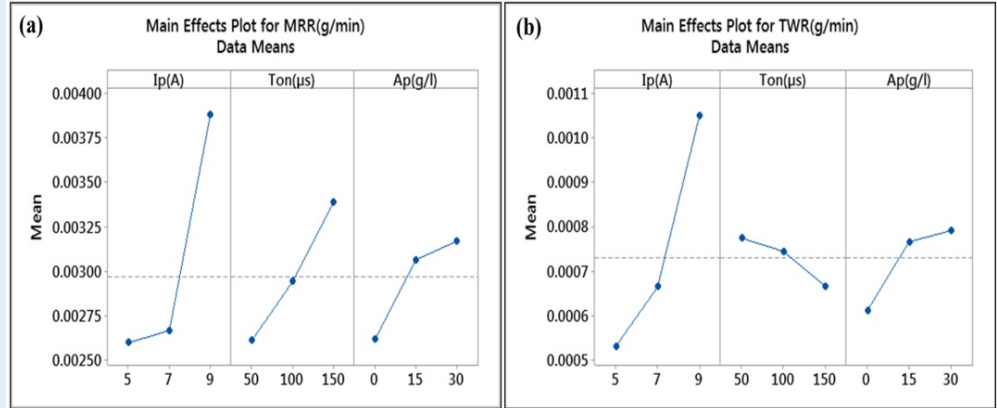


Figure 2: Main influence of process parameters on MRR and TWR: (a) MRR; (b) TWR.

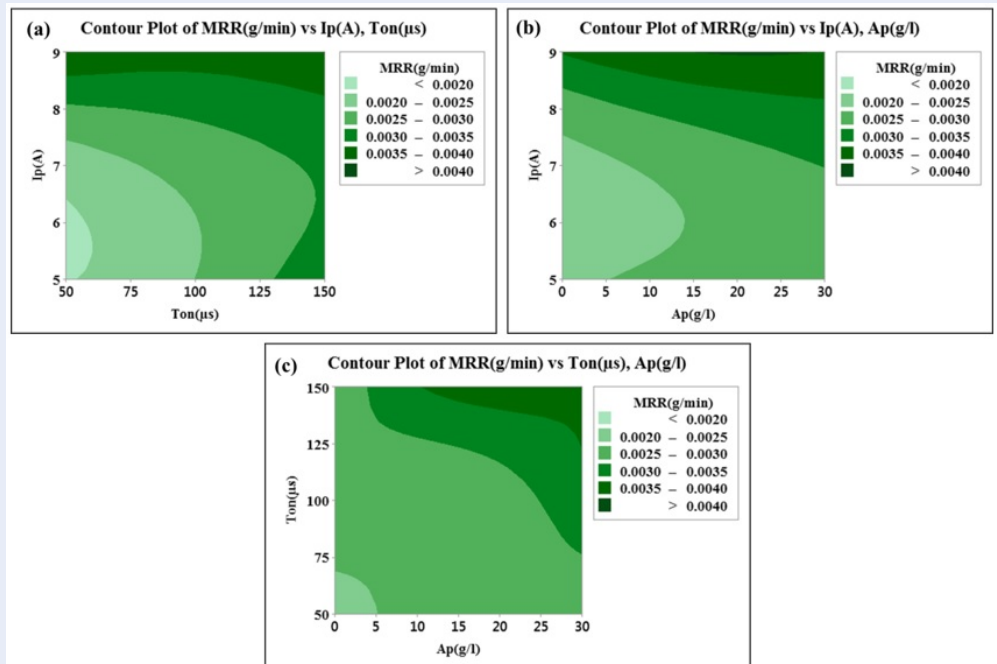


Figure 3: The incorporated influences of process parameters on MRR: (a) I_p and T_{on} , (b) I_p and A_p , and (c) T_{on} and A_p .

Table 5: Comparing between empirical values (EV) and predictive values (PV)

No.	TWR, g/min			MRR, g/min		
	PV	EV	Error (%)	PV	EV	Error (%)
16	0.0006934	0.000658931	4.97	0.0019772	0.001913934	3.2
17	0.0006347	0.000609828	3.92	0.0031653	0.003084515	2.55
18	0.0007405	0.000775432	4.71	0.0028395	0.002704641	4.75
19	0.0009483	0.000977515	3.08	0.0043135	0.004504535	4.43

Error(%)=Abs (PV-EV)/PV × 100%

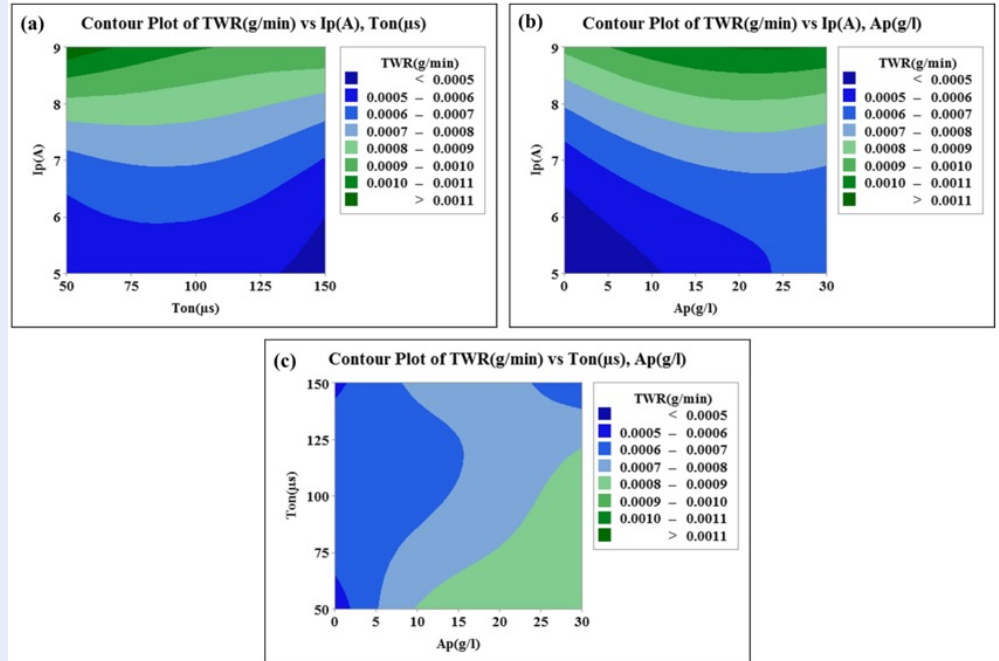


Figure 4: The incorporated influences of process parameters on TWR: (a) I_p and T_{on} , (b) I_p and C_p , and (c) C_p and T_{on} .

Optimization of the machining performance

In the PMEDM process, the machining performance is expected to meet the following criterion: the MRR is obtained at the maximum, while the TWR is acquired at the minimum. Hence, the issue of optimizing the machining performance is represented as follows:

When $x = [T_{on}, I_p, A_p]$ is found, the MRR and TWR simultaneously reach the minimum and maximum, respectively.

The process parameters were as follows: $50 \leq T_{on} \leq 150$ (μ s), $5 \leq I_p \leq 9$ (A), and $0 \leq A_p \leq 30$ (g/l).

This problem was resolved by applying gray relational analysis (GRA). The steps to perform the GRA are indicated in Figure 5:

All the GRC and GRG values corresponding to ranks are depicted in Table 6. The process parameters with the highest GRG (Rank 1) are selected for optimizing all the responses simultaneously (i.e., maximizing the MRR and minimizing the TWR). The optimal results are obtained as follows: $MRR_{max}=0.003397818$ (g/min) and $TWR_{min}=0.000481408$ (g/min) for the process parameter sets $I_p=5A$, $Ton=150 \mu s$, and $C_p=15$ g/l.

DISCUSSION

The accuracy of the MRR and TWR development models was considered via analysis of variance (ANOVA) with 95% confidence and 5% significance. Table 3 and Table 4 show the ANOVA results for RMR and TWR, respectively. The p value corresponding to the terms of the model is less than 0.05, which indicates that these terms of the model are significant. These terms are significant for the predictive model of MRR, comprising I_p^2 , $I_p \times T_{on}$, I_p , A_p , and T_{on} , while they are meaningful for the predictive model of TWR, comprising I_p^2 , and A_p^2 , $T_{on} \times A_p$, I_p , A_p , and T_{on} . The development models were verified by their adequacy/precision through coefficients, comprising “ R^2 ”, “ R^2 (pred)”, and “ R^2 (adj)”. The R^2 values for the MRR and TWR models are 0.9899 and 0.9918, respectively. This finding demonstrates good agreement between the experiential values and the predictive values. The “ R^2 (pred)” of these models (0.8504 for MRR and 0.8699 for TWR) is also a suitable compromise with the “ R^2 (adj)” (0.9716 for MRR and 0.977 for TWR). In addition, comparisons between the predicted values and experimental results are shown in Table 5. The small dislocations reveal that the regression models are suitable and can be employed for predicting responses with high precision.

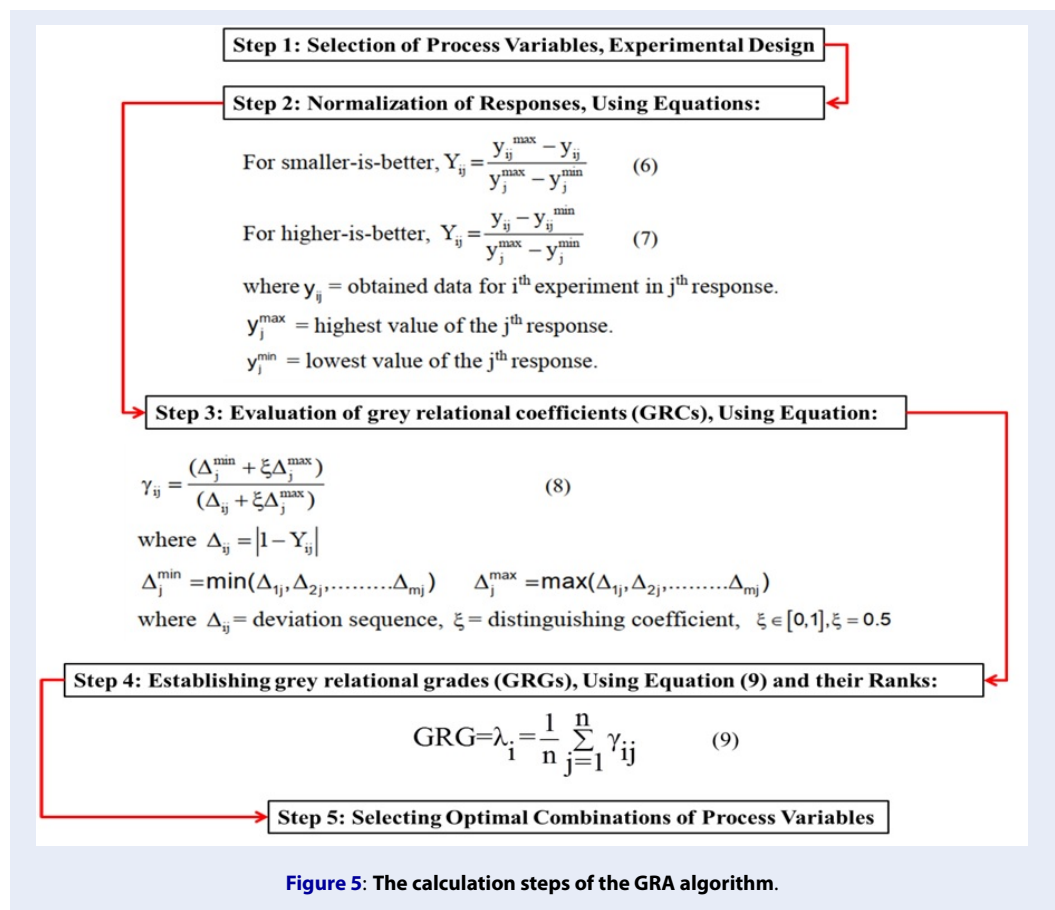


Figure 5: The calculation steps of the GRA algorithm.

Furthermore, these predictive models can be used to identify the optimum attributes.

Considering the influences of single factors and combined factors, **Figure 2a** reveals that A_p , I_p , and T_{on} have the same impact on the MRR. An increase in the MRR occurs when I_p , T_{on} , and C_p in the whole design space increase. This finding indicates that the MRR is ameliorated. Indeed, when I_p or T_{on} increase, thermal energy is generated in the discharge channel¹⁵⁻¹⁷. Furthermore, as the discharge zone expands, the conductive particles in the discharge channel are rooted¹⁸. This boosts the MRR. In **Figure 2b** shows the crucial impacts of the variables on the TWR. This indicates that the TWR increases with increasing I_p or C_p in the entire design space. Moreover, the increase in T_{on} in the entire design space reduces the TWR. In regard to the impact of the combined factors, see the **Figure 3a-c**, the MRR increases with increasing I_p for all the values of T_{on} and A_p (**Figure 3b-c**). 3a and b), and with a rise in T_{on} for all values of I_p and A_p (**Figure 3a** and c). In addition, the increase in A_p also causes an increase in the MRR for all values of I_p (**Figure 3b**) and for all val-

ues of T_{on} (**Figure 3c**). The MRR obtained the greatest value when A_p , T_{on} , and I_p achieved the highest values. The results for the combined impacts of the process variables on the TWR reveal that the TWR increases with increasing I_p for all values of T_{on} and A_p (**Figure 1**). 4a and b), and with an increase in A_p for all the values of I_p and T_{on} (**Figure 4b**). 4b and c). At the smallest values of T_{on} , I_p , and A_p , the TWR obtains the minimum value. From the abovementioned evaluation, it is clear that both I_p and/or T_{on} increase, causing the discharge energy to increase and leading to increases in the MRR and TWR^{19,20}. In addition, adding powder particles to the working liquid produces stratified discharge, which increases the MRR and decreases the TWR²¹. A combination of I_p and T_{on} leads to a low/high density of powder particles in the next discharge. This has a positive/negative influence on the improvement in MRR and TWR.

The optimization results are obtained via the GRA algorithm. To confirm the correctness of the algorithm for predicting optimal results. The values of MRR and TWR obtained by experiment at the optimum process parameters are presented in **Table 7**

Table 6: GRA for MRR and TWR

Run	GRCs		GRG	
	MRR	TWR	Value	Rank
1	0.9839306	0.3333333	0.6586320	6
2	0.3333333	0.6947430	0.5140381	11
3	0.9614190	0.3592588	0.6603389	5
4	0.4456508	0.5576316	0.5016412	12
5	0.4349637	0.5674689	0.5012163	13
6	1.0000000	0.3940663	0.6970332	2
7	0.3995779	0.4909593	0.4452686	15
8	0.4332881	0.6135046	0.5233963	10
9	0.3348458	0.7557299	0.5452879	9
10	0.6814166	0.4253023	0.5533594	8
11	0.6846263	0.6567425	0.6706844	4
12	0.3789070	1.0000000	0.6894535	3
13	0.4244016	0.5615576	0.4929796	14
14	0.4187524	0.7029110	0.5608317	7
15	0.6237927	0.8435539	0.7336733	1

and are compared with the values of the output attributes according to the predictive models that are within the tolerable assortment. The maximum and minimum errors are 4.15% for the TWR and 1.5% for the MRR, respectively. This confirms that the optimal results are consistent. In addition, to gain further insight into the optimal results, several surface attributes were explored and compared. Microcracks, droplets, voids, and globules of debris are called microdefects on surfaces. In **Figure 6**, A comparison of the microdefects in the optimum electrical mode was conducted between powder mode (**Figure 6a**) and in the no-powder mode (**Figure 6b**). It is clear that the surface obtained with the powder mode has fewer microcracks, voids, and droplets and smaller globules of debris than the surface obtained with the powderless mode.

In this study, the machining performance of heat-treated SKD61 steel by an EDM process with a tungsten powder alloy was investigated. Evaluation of the influence of process parameters on machining performance, establishment of a prediction model for machining performance, and optimization of process parameters were carried out. The following principal conclusions have been drawn:

- Regression models were established, and ANOVA was performed to evaluate the pre-

cision of these development models (MRR and TWR). The outcomes indicated that the regression models have high precision and can be utilized to investigate the influences of process variables on machining performance and to predict the desired MRR and TWR in the entire design space.

- The optimal responses and process variables, including an MRR_{max} of 0.003397818 (g/min), a TWR_{min} of 0.000481408 (g/min), a peak current of 5 (A), a pulse-on time of 150 (μ s), and a powder concentration of 15 (g/l), were found through the RSM-GRA methodology.
- In addition, the number of microdefects on machined surfaces determined by PMEDM is better than that on machined surfaces determined by EDM at the optimum electrical parameters.
- Moreover, the prediction method of this study could be utilized for machining performance prediction for other steel alloys.
- In future works, surface features such as the thickness of the recast layer, percentage of microcracks on surfaces, and surface topography of heat-treated SKD61 steel will be investigated for the applicable manufacturing industry.

Table 7: Verification experiments of the results at the optimal process parameters

Machining attributes	Optimum process parameters	EV	PV	Error (%)
TWR(g/min)	$I_p = 5A, T_{on} = 150\mu s, C_p = 15 \text{ g/l}$	0.000501408	0.000481408	4.15
MRR(g/min)		0.00334667	0.003397818	1.5
Error (%) = Abs (PV – EV)/PV × 100%				

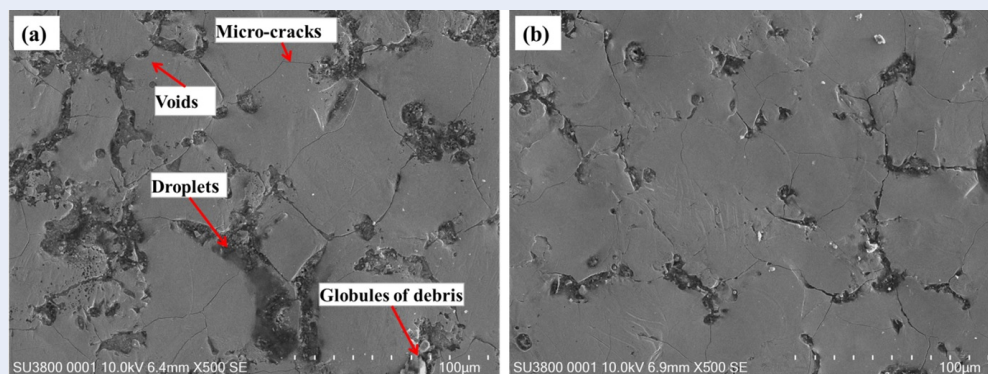


Figure 6: Microdefects on surfaces: (a) at optimal process parameters without powders; (b) at optimal electrical parameters with powders.

LIST OF ABBREVIATIONS

- EDM: Electronecharge Machining
- PMEDM: Powder Mixed Electrodischarge Machining
- MRR: Material removal rate
- TWR: Tool wear rate
- ANOVA: Analysis of variance
- GRA: Gray relational analysis
- SR: Surface roughness
- MH: Microhardness
- RSM: Response surface methodology
- EV: Empirical values
- PV: Predictive values
- GRC: Gray relational coefficient
- GRG: Gray relational grade

COMPETING INTERESTS

The authors declare that they have no conflicts of interest.

ACKNOWLEDGMENTS

This research is funded by the Vietnam National Foundation for Science and Technology Development (NAFOSTED) under grant number 107.99-2021.29.

AUTHORS' CONTRIBUTIONS

Van-Tao Le: Proposal and designed study; Van-Tao Le, Tien Long Banh, Thi Hong Minh Nguyen, Tien

Dung Hoang, Van Thuc Dang , Hoang Cuong Phan: Performed experiments, Wrote and prepared the original manuscript; Van-Tao Le, Tien Long Banh, Thi Hong Minh Nguyen, Tien Dung Hoang: Reviewing and Editing. All authors read and approved the final version of the manuscript for publishing.

REFERENCES

1. Philip JT, Mathew J, Kuriachen B. Transition from EDM to PMEDM - Impact of suspended particulates in the dielectric on Ti6Al4V and other distinct material surfaces: A review. *J Manuf Process.* 2021;64:1105-42; Available from: [https://doi:10.1016/j.jmapro.2021.01.056](https://doi.org/10.1016/j.jmapro.2021.01.056).
2. Ishfaq K, Rehman M, Wang Y. Toward the Targeted Material Removal with Optimized Surface Finish During EDM for the Repair Applications in Dies and Molds. *Arab J Sci Eng.* 2023;48(3):2653-69; Available from: [https://doi:10.1007/s13369-022-07006-x](https://doi.org/10.1007/s13369-022-07006-x).
3. Erden A, Bilgin S. Role of Impurities in Electric Discharge Machining. In: *Proceedings of the Twenty-First International Machine Tool Design and Research Conference.* Macmillan Education UK; 1981:345-50; Available from: [https://doi:10.1007/978-1-349-05861-7_45](https://doi.org/10.1007/978-1-349-05861-7_45).
4. Srivastava S, Vishnoi M, Gangadhar MT, Kukshal V. An insight on Powder Mixed Electric Discharge Machining: A state of the art review. *Proc Inst Mech Eng Part B J Eng Manuf.* 2022;9544054221111896; Available from: [https://doi:10.1177/09544054221111896](https://doi.org/10.1177/09544054221111896).
5. Askeland DR. *The Science and Engineering of Materials.* Springer US; 1996; Available from: <https://doi.org/10.1007/978-1-4899-2895-5>.

6. Banh LT, Nguyen PH, Ngo C. Tool wear rate optimization in PMEDM using titanium powder by Taguchi method for die steels. *Sci Technol Dev J.* 2016;19(2):88-97; Available from: <https://doi:10.32508/stdj.v19i2.656>.
7. Huu PN. Study of the effects of process parameters on tool wear rate in powder mixed electrical discharge machining by Taguchi method. *Sci Technol Dev J.* 2018;20(K7):55-60; Available from: <https://doi:10.32508/stdj.v20iK7.1375>.
8. Hu P, Ying L, He B. *Hot Stamping Advanced Manufacturing Technology of Lightweight Car Body.* Springer Singapore; 2017; Available from: <https://doi.org/10.1007/978-981-10-2401-6>.
9. Wu KL, Yan BH, Huang FY, Chen SC. Improvement of surface finish on SKD steel using electrodischarge machining with aluminum and surfactant added dielectric. *Int J Mach Tools Manuf.* 2005;45(10):1195-201; Available from: <https://doi:10.1016/j.ijmachtools.2004.12.005>.
10. Yan B, Lin Y, Huang F, Wang C. Surface Modification of SKD 61 during EDM with Metal Powder in the Dielectric. *Mater Trans.* 2001;42(12):2597-604; Available from: <https://doi:10.2320/matertrans.42.2597>.
11. Le VT. The role of electrical parameters in adding powder influences the surface properties of SKD61 steel in EDM process. *J Brazilian Soc Mech Sci Eng.* 2021;43(3):120; Available from: <https://doi:10.1007/s40430-021-02844-6>.
12. Le VT. Influence of Processing Parameters on Surface Properties of SKD61 Steel Processed by Powder Mixed Electrical Discharge Machining. *J Mater Eng Perform.* 2021;30(4):3003-23; Available from: <https://doi:10.1007/s11665-021-05584-9>.
13. Bezerra MA, Santelli RE, Oliveira EP, Villar LS, Escalera LA. Response surface methodology (RSM) as a tool for optimization in analytical chemistry. *Talanta.* 2008;76(5):965-77; Available from: <https://doi:10.1016/j.talanta.2008.05.019>.
14. Tao Le V. The influence of additive powder on machinability and surface integrity of SKD61 steel by EDM process. *Mater Manuf Process.* 2021;36(9):1084-98; Available from: <https://doi:10.1080/10426914.2021.1885710>.
15. Le VT. An investigation on machined performance and recast layer properties of AISI H13 steel by Powder Mixed-EDM in fine-finishing process. *Mater Chem Phys.* 2022;276:125362; Available from: <https://doi:10.1016/j.matchemphys.2021.125362>.
16. Kunieda M, Lauwers B, Rajurkar KP, Schumacher BM. Advancing EDM through Fundamental Insight into the Process. *CIRP Ann Manuf Technol.* 2005;54(2):64-87; Available from: [https://doi:10.1016/S0007-8506\(07\)60020-1](https://doi:10.1016/S0007-8506(07)60020-1).
17. Le V tao. New insights into the surface features of SKD61 steel at heat-treated and non-heat-treated states as processed by powder-mixed EDM. *Mater Lett.* 2023;352:135199; Available from: <https://doi:10.1016/j.matlet.2023.135199>.
18. Furutania K, Saneto A, Takezawa H, Mohri N, Miyake H. Accretion of titanium carbide by electrical discharge machining with powder suspended in working fluid. *Precis Eng.* 2001;25(2):138-44; Available from: [https://doi:10.1016/S0141-6359\(00\)00068-4](https://doi:10.1016/S0141-6359(00)00068-4).
19. Ho K, Newman S. State of the art electrical discharge machining (EDM). *Int J Mach Tools Manuf.* 2003;43(13):1287-300; Available from: [https://doi.org/10.1016/S0890-6955\(03\)00162-7](https://doi.org/10.1016/S0890-6955(03)00162-7).
20. Le VT, Hoang L, Ghazali MF, et al. Optimization and comparison of machining characteristics of SKD61 steel in powder-mixed EDM process by TOPSIS and desirability approach. *Int J Adv Manuf Technol.* 2023;(123456789); Available from: <https://doi:10.1007/s00170-023-12680-8>.
21. Ekmekci B, Yaşar H, Ekmekci N. A Discharge Separation Model for Powder Mixed Electrical Discharge Machining. *J Manuf Sci Eng.* 2016;138(8):1-9; Available from: <https://doi:10.1115/1.4033042>.